Proceedings Paper:
Tonge, A, Usher, S, Peakall, J et al. (7 more authors) (2019) Use of In Situ Acoustic Backscatter Systems to Characterize Spent Nuclear Fuel and its Separation in a Thickener. In: WM2019 Conference Proceedings. Waste Management Symposium 2019, 03-07 Mar 2019, Phoenix, Arizona. WM Symposia . ISBN 978-0-9828171-9-3

Use of In Situ Acoustic Backscatter Systems to Characterize Spent Nuclear Fuel and its Separation in a Thickener-19288

Alastair Tonge*, Shane Usher**, Jeff Peakall,***, Steven Freear****, David Cowell****, George Franks**, Krishna Mohanarangam*****, Vivek Ravisankar*****, Martyn Barnes****** and Timothy Hunter*

*School of Chemical and Process Engineering, University of Leeds, Leeds LS2 9JT, UK

**Department of Chemical Engineering, The University of Melbourne, Melbourne 3010, Australia

***School of Earth and Environment, University of Leeds, Leeds LS2 9JT, UK

****School of Electronic & Electrical Engineering, University of Leeds, Leeds LS2 9JT, UK

***** CSIRO Mineral Resources, Western Precinct, Research Way, Clayton 3168, Australia

******Sellafield Ltd, Hinton House, Warrington WA3 6GR, UK

Abstract

To aid in the transportation, dewatering and storage of radioactive UK legacy waste sludges at Sellafield Ltd., the application of an Acoustic Backscatter System (ABS) was investigated in this study, as a method for monitoring suspended solids concentration and consolidation of cohesive and aggregated sludges (that form the basis of many wastes at Sellafield). An ABS represents a particularly promising technology, as they can be used with minimal intrusion, to measure both particle size and concentration depending on prior system knowledge, through inversion of the return echo voltage response of pulse-echo signals in the MHz range.

To assess the application for continuous, high concentration (~30 % v/v) thickened wastes, an ABS was utilised to characterise a pseudo-steady state laboratory thickener over hours, using flocculated calcite as a representative test material. Measurements were taken both horizontally through a consolidated bed using a 1 MHz transducer and vertically downwards with a 2 MHz transducer to measure sediment concentration above the settled bed and track bed height via the interface reflection. Characterisation of flocculated aggregate diameters was initially determined to be ~510 µm, using an inline Focussed Beam Reflectance Measurement (FBRM) device. The submerged 2 MHz probe indicated that there were only limited changes to the dispersion concentration or size over time. Changes in settled bed density, due to increasing bed height and changes in the underflow flow rate, were qualitatively measured via differences to the acoustic signal attenuation over time. An initial increase in attenuation with bed height was observed as the bed densified due to local compression. Once an equilibrium bed height was reached, the acoustic attenuation remained fairly constant with time, although the bulk underflow density was reduced with the increase in underflow rate. The solids residence time in the bed, determined from a transitive volume-balance model, was found to be ~3200 s for pseudo-steady state operation at a maintained bed height of ~0.175 m. Results of the study highlight the potential the ABS as a remote process monitoring tool for both relatively dilute suspensions and concentrated thickened mineral sludges, with potential applications across waste processing sites at Sellafield.

Introduction

The Pile Fuel Storage Pond (PFSP) was built in 1949/50 at Sellafield for receipt and storage of fuel and isotopes from the two Windscale Pile reactors as well as the de-canning of fuel elements prior to reprocessing. The pond was linked through submerged water ducts to the reactors along which fuel and isotopes were transferred after discharge into skips, and provided a cooling zone where the fuel could be de-canned while submerged [1]. Following the construction of the First Generation Magnox Storage Pond (FGMSP) in 1962, the PFSP was used to store miscellaneous Intermediate Level Waste (UK) and fuel for which no defined disposal route was available. The contained inventory within it is therefore complex, ranging from highly mobile low-density organic sludge, inorganic material such as debris from fuel and metal corrosion, wind-blown debris, algae, bird guano and reactor furniture with almost 1000 waste forms identified on the plant inventory[1, 2].

Due to the large cost for storage and processing of these waste sludges and because of the high risk of radiological or toxicological contamination, there is a strong motivation for clean-up and reprocessing of the legacy nuclear waste inventories at Sellafield. To collect the sludge within the PFSP an 'in pond' corral was used to allow for an early start on desludging by concentrating the sludge. Much research has been directed towards developing technologies for the remote characterization of nuclear waste for application at sites such as the PFSP, FGMSP and other mobilisation, transport and storage processes at Sellafield [3, 4]. The ABS represent such a technology, as they can be used with minimal intrusion to measure both particle size and concentration depending on prior system knowledge in opaque suspensions where light based techniques would not be possible [5]. As ABS probes are typically only a few centimetres in diameter, they may be mounted on the outside of pipes and tanks and typically have several operating frequencies that are adjusted to suit the chosen system.

A critical aspect of legacy waste processing at Sellafield, is an understanding of potential volume consolidation upon transfer to interim storage. Indeed, the dewatering of cohesive sediment suspensions is of great interest more generally to minerals, wastewater processing and nuclear industries, where storage and packaging costs are high and so minimisation of waste volume is crucial. The ability to model these systems as a function of parameters such as rake speed, aggregate size and, of concern in this paper, bed density, has therefore been studied extensively through both semi-empirical settling models and CFD modelling of flocculation, aggregation and settling dynamics within thickener operations [6-11]. The application of various sludge blanket and particle concentration measurement techniques [12] such as X and γ-ray absorption [13] and conductivity and light based measurements [14] have thus been studied in previous reported literature. However, many of these are limited, either by their cost, the scale of the process they may be applied to or by the solids fraction range that is able to be monitored [15].

To date, ABS studies on these types of consolidated sludge systems are limited. Nevertheless, concentration inversion models exist for both low (up to ~150 gl^{-1}) [5, 16, 17] and high concentration (up to ~30 % v/v) [18] suspensions, provided certain acoustic parameters such as the velocity of sound in the solid and particle characteristics such as size are known or can be estimated. Limitations in these models exist, however, due to either error propagation with increased measurement depth [5] or the need to model particle acoustic properties where sampling is limited and particle acoustic properties cannot be assumed *a priori* [18]. Moving toward a more qualitative analysis, ABS attenuation measurements for determining bed density have been demonstrated previously by Hunter *et al.* [19] in the same laboratory-scale thickener used in this study. It was found that, although attenuation measurements were not depth-independent vertically through the bed, response at fixed depths for the same bed height could be qualitatively correlated to changes in concentration over time [20].

By taking horizontal measurements through the bed, as is detailed in this paper, attenuation determined while keeping the measurement zone fixed at a single height rather than across a range of heights, eliminated bed depth influence when determining the attenuation value. If sediment concentration through the hindered settling zone and in the compressed bed can be determined on-line, then detailed aggregation models such as those employed by Usher *et al.* [7, 9] can be used to optimise solid-liquid separation by increasing the underflow concentration or the solids flux through the thickener by altering operational parameters such as the rake speed and underflow flowrate to control the bed height and solids residence time [21]. Coupling this system with in-line particle size data, collected on devices such as a Focussed Beam Reflectance Monitor (FBRM) [22]–[24], would allow for CFD models, such as that proposed by Heath and Koh [11], to be compared simultaneously with *in situ* measurements [7]–[10] to allow for real-time monitoring and optimisation of waste transport processes at Sellafield.

Development of an ABS for remote, real-time monitoring of waste processing and separation in dewatering processes will bring significant improvements to waste management efficiency and model predictions of these systems in operational environments. However, while there is high potential applicability of ABS technology in the nuclear waste sector, currently there is very little data available on the application of ABS to fine cohesive and aggregated sludges, particularly at high solids concentrations, which form the basis of many wastes encountered at Sellafield. This lack of system data greatly limits the current utilization of acoustics in real industrial applications. This study therefore attempts to infer changes in the settled bed density of a laboratory scale thickener as a function of bed height and underflow flow rate through simultaneous ABS measurements both horizontally through the bed and vertically downward through the settling zone. The solids residence time and underflow concentrations are modelled based on bed height measurements taken with the ABS and a modified mass balance from Bürger, Diehl and Nopens [25] (See Materials and Methodology). Underflow concentration values from the model are then compared to those from underflow sampling at 15-minute intervals for a flocculated calcite sediment system.

Materials and Methodology

Omyacarb 2 calcite (d_{50} approximately 2 microns) was chosen as a simulant material for SNF in this study as it has been used previously for ABS studies in both the same laboratory scale thickener [19] and in large scale settling trials [26]. Its polymer flocculation and settling dynamics have also been studied extensively [22, 27, 28, 29] and are of great interest for mining and waste processing operations involving limestone or marble.

ABS measurements were performed in a laboratory scale thickener at the University of Melbourne, to assess the application of the ABS as a real-time monitoring device for high concentration (~30 % v/v) solid-liquid separation, such as potentially encountered during nuclear waste dewatering processes. Figures 1 and 2 show a schematic for the laboratory scale thickener used and the placement of the ABS probes. The inlet pipe provided a total flocculation length of 6 m prior to the feedwell. The settling zone was a Perspex column ~1 m high and 0.3 m diameter, shown in Figures 2(a) and (b), with a fitted metal cone for underflow discharge accompanied by two scraper rakes (1 x 1 cm), shown in Figure 2(c) that rotated radially from a central mixing rod. An aqueous calcite feed, diluted in-line with mains tap water from a 50 %w/w slurry, at a nominal ~4 %w/w concentration was pumped at 105 L/hr in-line with a 2000 ppm aqueous, high molecular weight, anionic polymer solution (AN934SH, SNF Chemicals) so as to produce 200 g polymer t^{-1} solid in the mixed inlet feed. A mean pipe velocity of 0.389 m/s was achieved along the 6 m of pipe length before entering the feedwell of the thickener (Figure 2(d)) allowing for flocculation under moderate turbulent conditions to occur, in order to create a highly flocculated suspension, typical of mineral wastes.

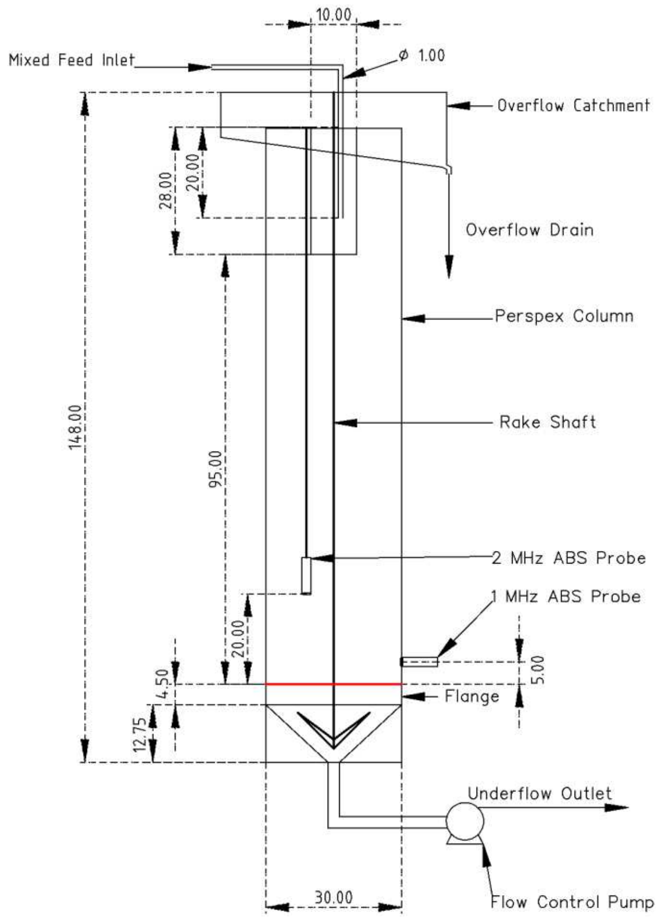

Figure 1 Laboratory-scale thickener column diagram (measurements are in centimetres). The bold red line indicates the top of the flange, the zero height from which the probe heights are referenced.

By careful operation of the pump at the tank outlet, pseudo-continuous operation of the thickener was achieved after the consolidated sediment bed had been allowed to build-up to an equilibrium height of ~0.175 m. Once the desired bed height was reached the underflow rate was gradually increased and set to achieve steady-state (constant bed height) operation of the tank. The volume of feed allowed for ~5 hours of continuous operation.

Acoustic measurements were taken using a commercial Aquascat1000 (Aquatec Group Ltd., UK) with 1 and 2 MHz transducers, where the 1 MHz probe was positioned horizontally through the settled bed at 5 cm above the top of the column flange and the 2 MHz probe was positioned facing vertically downward 20 cm above the initial column base (See Fig. 1). The 2 MHz probe was periodically moved upward, as the consolidated bed built up over time, to ensure that the first 0.1 m of the 0.3 m measurement zone was in the settling zone directly above the bed. The vertical probe allowed for tracking of the sediment bed height via the interface reflection of the acoustic signal as well as indicating any changes in the particle size or concentration in the settling zone above the bed throughout the trial. The horizontal probe allowed for continuous qualitative measurement of changes in settled bed density from bed height and underflow rate changes, via attenuation of the backscattered acoustic signal, as demonstrated in previous work by Hunter *et al* [19].

Figure 2 a) Overall view of the setup used for the laboratory-scale thickener experiments, b) the observed flocs during operation, c) the rake and funnel section, and d) the feedwell.

The size of the flocculated aggregates at the column inlet were estimated using online measurements from a Focussed Beam Reflectance Measurement probe (Lasentec/ Mettler-Toledo), taken in a once-through flow system (total flocculation length of 5.34 m and a pipe internal diameter of 7.7 mm) designed to mimic the shear conditions and nominal sediment and polymer concentration used for the thickener experiments (~4 % w/w calcite and 195 gt^{-1} (solid) with a flocculation length of 6 m and a hydraulic pipe diameter of 10 mm). The pressure drop and hence the energy dissipation rate was calculated using the Blausius friction factor, from which the shear rate could then be found as per the method used by Heath *et al.* [29]. The initial flow rate of the slurry in the pipe reactor was therefore calculated such that the product of the shear rate and residence time in the pipe reactor and the thickener feedwell were of similar values (dimensionless values of 5616 for the thickener versus 5900 for the pipe reactor) while still keeping the flow rate high enough to suspend the flocs in the pipe and get sufficient counts from the FBRM to obtain a statistically accurate particle size measurement.

The FBRM provides particle size measurement by having a laser rotate at a set speed as particles pass by the focal plane. As the laser crosses the interface, the laser is backscattered until it reaches the opposing edge of the particle and so multiplying this time period by the scan speed will give a distance corresponding to the chord length across the particle [15]. For a spherical particle, the laser chord will intersect the particle at lengths less than the diameter many times more often and so inversion algorithms, such as those proposed by Li and Wilkinson [30, 31] have been developed by fitting a modelled chord length distribution (CLD) from an initially estimated particle size distribution (PSD) to the experimental CLD collected with the FBRM. Empirically, a square-weighted chord length distribution has been seen to agree well with other particle size measurement techniques for 50 – 400 µm and from 0.1 – 20 % w/v and is commonly used to both qualitatively and quantitatively measure the extent of flocculation [23, 24, 32].

In order to model the solids residence time and outlet concentration from the thickener as a function of measured bed height a volume balance was performed between the outlet and the top of the settled bed detailed below. Within the thickening zone the increase of mass per unit time in an arbitrary interval between two heights (z_1, z_2) is given by Bürger, Diehl and Nopens [25] as

$$\frac{d}{dt}\int_{z1}^{z2} AC(z,t)dz = A(\phi_{z1} - \phi_{z2}) + \int_{z1}^{z2} Q_f(t)C_f(t)\delta(z)dz \qquad 1$$

where the first term represents the mass accumulation with time (t) given by the cross-sectional area, A, and the integral of concentration with respect to height over the interval width. The second term represents the sediment mass flux in and out $(\phi_{z1} - \phi_{z2})$ due to the downward velocity caused by both the underflow and hindered settling/ compression of the bed. The third term represents the contribution of the feed to the mass accumulation in the interval given by the feed flow rate (Q_f), concentration (C_f), defined as the solids volume fraction multiplied by the solid density, and the Dirac delta distribution (δ). The sediment flux term (ϕ) is given by [25] as

$$\phi\left(C, \frac{\partial C}{\partial z}, z, t\right) = v_{hs}(C)C + \frac{Q_u(t)C}{A} - (\, d_{comp}(C) + d_{disp}(z)\,)\frac{\partial C}{\partial z} \qquad 2$$

where d_{comp} is the reduction to the hindered settling velocity (v_{hs}) due to the effective solids stress of the network that occurs when the bed concentration exceeds the gel point and the bed forms a cohesive network, while d_{disp} represents dispersion effects. Both terms are expressed in a form analogous to Fick's first law of diffusion, in terms of a concentration gradient $\partial C/\partial z$. If the balance is performed at the surface of the bed the sediment flux-in term (ϕ_{z1}) would be 0 as there is no bed above this point to cause a flux and only the contribution from the feed would cause mass accumulation. Setting $\phi_{z1} = 0$ and dividing equation **1** by A and C we obtain

$$\frac{d}{dt}\int_{z1}^{z2} dz = \left(-\frac{\phi_{z2}}{C(t)}\right) + \int_{z1}^{z2} \frac{Q_f(t)C_f(t)}{C(t)A}\,\delta(z)dz \qquad 3$$

By performing the integration and substituting equation **2** into equation **3** the change in height of the top layer of the bed $(z2)$ from a reference point $(z1)$ (defined here as h_{bed}) at each time step (dt) can be defined:

$$\frac{dh_{bed}}{dt} = -\frac{Q_u(t)C}{A} - \left[v_{hs}(C) - (\, d_{comp}(C) + d_{disp}(z)\,)\frac{\partial C}{\partial z}\right] + \int_{z1}^{z2} \frac{Q_f(t)C_f(t)}{C(t)A}\,\delta(z)dz \qquad 4$$

$$\int_{z1}^{z2} \delta(z)dz = 1 \qquad 5$$

As the effective solids stress of the network is not known the hindered settling, compression and dispersion terms were collected into a single parameter $(dh\_compression)$ such that

$$dh_{compression} = -\left[v_{hs}(C) - (\, d_{comp}(C) + d_{disp}(z)\,)\frac{\partial C}{\partial z}\right] \qquad 6$$

dh_{bed} was measured in this experiment by the vertically facing 2 MHz ABS probe and the feed and underflow were known at all time steps.

Therefore, using MATLAB, a transitive volume balance model between the top of the bed and the top of the underflow cone was set up such that the thickness of each newly settled layer (*dz)* is given by:

$$dz = \frac{\left(\frac{C_{feed} * Q_{feed}}{C_z}\right)}{A_{tank}} \quad 7$$

Where C_{feed} is the feed concentration (in w/v), Q the flowrate, C_z the settled layer concentration and A_{tank} the cross-sectional area of the tank. The value of C_z was adjusted so that the output concentration from the model (shown below) matched the values determined from sampling. The change in height due to compression of the bed at each time step (i) can be given in terms of the model parameters:

$$dh(i)_{compression} = dh(i)_{bed} + \frac{dt * Q(i)_u}{A_{tank}} - dz \quad 8$$

Where $dh(i)_{bed}$ is the change in height of the bed at each time step as measured by the ABS and dt is the value of the time step. As a new layer j_n lands at each time step the position of the layer j_n is given by:

$$z(j_n, i) = h(i)_{bed} \quad 9$$

where $h(i)_{bed}$ is the height of the bed at each time step. The new position of the already settled layers (j_1... j_{n-1}) at each time step is then given by.

$$z\,(j1 \ldots jn-1, i\,) = z\,(j1 \ldots jn-1, i-1\,) - \frac{Q(i)_u dt}{A_{tank}} + dh(i)_{compression} \quad 10$$

The residence time corresponding to each layer at each time step can then be calculated as follows.

$$t_{res}(j1 \ldots jn-1, i\,) = t(i) - t(j1 \ldots jn-1, i\,) \quad 11$$

Completing the volume balance at the outlet, as the total downward velocity of the layers is known from $\frac{dt*Q(i)_u}{A_{tank}} - dh(i)_{compression}$ the predicted mass flow and concentration at the outlet is given by;

$$m_{out} = \left(\frac{dt * Q(i)_u}{A_{tank}} - dh(i)_{compression}\right) A_{tank} C_z \quad 12$$

Dividing by $Q(i)_u$ the concentration (w/v) at the outlet can then be found

$$C_{out} = \left(\frac{dt}{A_{tank}} - \frac{dh(i)_{compression}}{Q_u}\right) A_{tank} C_z \quad 13$$

Results and Discussion

Figure 3 shows FBRM data for the conditions used in the pipe flow reactor that most closely mimicked those at the thickener feed outlet.

Although the particle size is seen to decrease slightly with time the change is not significant and is likely due to small fluctuations in flocculant and slurry feed rate and concentration. The mean value for the square-weighted chord length, demonstrated previously by other authors to be a good measure of flocculated particle size calculated from a chord length distribution [23, 32], was 512.7 µm. Although the particle size observed here is large compared to those seen by other authors it should be noted that the flocculant dose was much higher (200 g of flocculant per tonne of solids compared to 20 g t^{-1} used by Heath *et al.* [29]) and from visual inspection of the flocs in the tank (Figure 2(c)) this value seems reasonable.

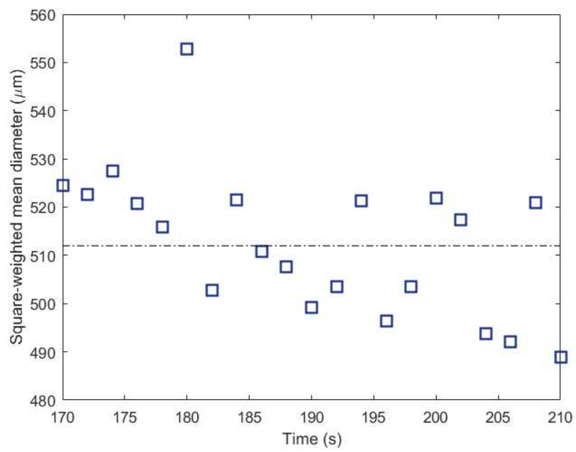

Figure 3 FBRM square-weighted chord length data obtained from flow reactor for shear conditions corresponding to laboratory scale thickener feed shear history. Dot-dash line shows mean value.

Figures 4 (a) and (b) show time averaged decibel signals at different times over the course of the trial for the 1 and 2 MHz probes with signals averaged over 15- and 1-minute intervals respectively. At all times shown, the profiles appear qualitatively similar. For the horizontal 1 MHz data, at very small distances (<0.03 m) the signal is complicated by ringing interference from the Perspex wall, and is ignored in analysis. After this point, the signal decays in an approximately linear fashion with distance, until reaching the noise floor of the instrument. The g radient of the decibel profiles between 0.03 and 0.06 m from the probe were used to approximate the bed attenuation (in db/m) and was observed to increase for later times (>3300 s) whereupon it remained relatively constant during steady-state operation (~9000-14000 s). The backscatter profiles for the vertically mounted 2 MHz profiles (Figure 4 (b)) are seen to remain relatively constant throughout the course, indicating the inlet particle concentration and aggregate sizes did not significantly change during the experiment. Here, the signal peak at very small distances (<0.02 m) is due to ringing interference from the probe itself, whereas after this point, the signal decays in a more logarithmic fashion, due to the much lower concentration in the dispersion zone above the bed. The logarithmic decay is seen because, at low particle concentrations, additional signal components from scattering are significant compared to the attenuation signal components causing the relationship to appear logarithmic. At high particle concentrations however, due to the general increase of the attenuation signal with particle concentration[18]–[20] these scattering components are not seen to have as significant an effect on the signal-distance relationship and the signal appears more linear. This change in the signal-distance relationship with concentration has also been observed by Hunter *et al.* for spherical glass particle dispersions up to 50 g l^{-1} [20]. An example of a reflection peak used to determine the bed height can be seen in Figure 4 (b).

The probe was moved in order to try maintain at least 10 cm between the probe and top of the bed, hence this peak is not seen to be as close at later time steps, despite the bed height actually increasing.

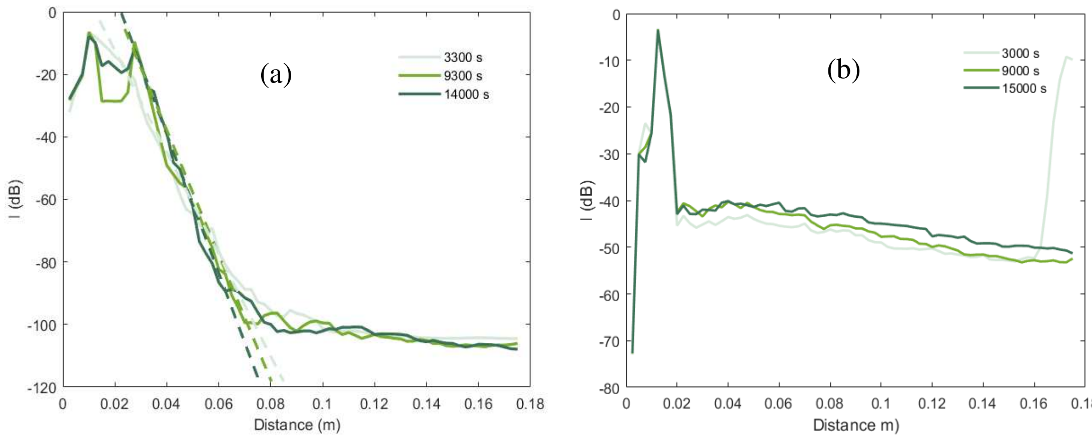

Figure 4 a) Backscatter strength vs distance for a) horizontally mounted 1 MHz probe (averaged over 15 minutes, dashed lines indicate attenuation fits), and b) vertically mounted 2 MHz probe (averaged over 1 minute)

Figure 5 (a) shows the bed height as determined from the bed reflection using the vertically mounted 2 MHz ABS probe and the visually determined height at the edge of the tank. The secondary y-axis shows the underflow rate at all stages during the experiment. The initial value for the underflow rate corresponded to one third of the concentrated slurry feed rate in order to allow a bed to form in the thickener. As the observed bed height approached 15 cm at around 4920 s the underflow rate was increased gradually and set to maintain the thickener at steady state operation, such that the bed height would remain constant. The final value set for the underflow rate was ~ 20% higher than the slurry feed rate to account for lower solids concentration in the underflow.

The initial period after turning the underflow pump up to its final value maintained a relatively constant bed height. However, the bed height seen by the ABS gradually decreased while the visual height measurement increased from ~13000 seconds onward. It was assumed this change was caused by “ratholing” of the bed. “Ratholing” or “coring” is where the centre of the bed collapses due to the excessive underflow creating a channel through which thinner sludge can be pulled from above [33].Good agreement was seen between the height determined from the bed reflection using the ABS and the visually determined height. Sediment was seen to pile in the centre of the tank as the bed built up causing a larger reading for the height of the bed to be measured with the ABS for most of the experiment. Due to the potential change in slope of the bed formed over time, it was not possible to eliminate the error reliably, although for most of the time, the off-set between the two measurement techniques was relatively constant (suggesting minimal changes to the slumping angle) before ratholing occured toward the end of the experiment.

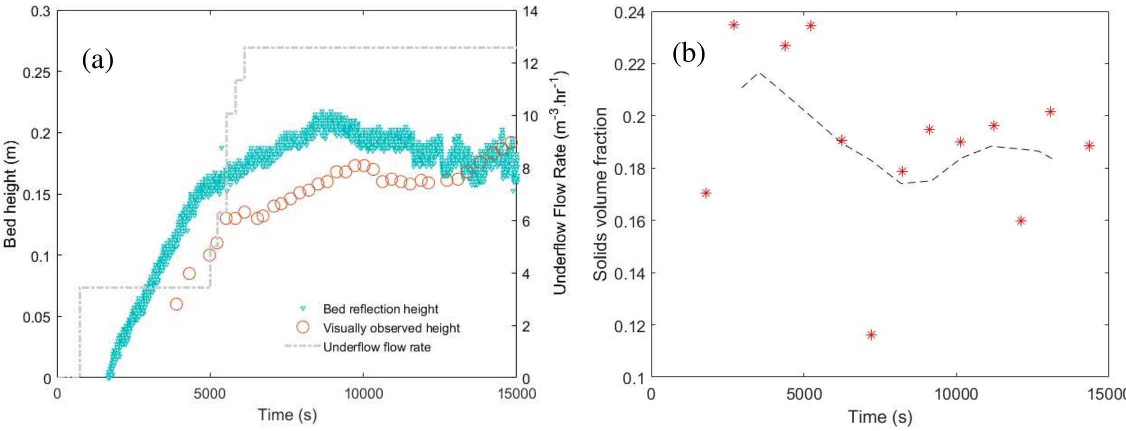

Figure 5 a) bed height as measured with the ABS backscatter and visual measurements with underflow flow rate vs time, and b) underflow sample data (solids volume fraction) vs time

Figure 5 (b) shows underflow sample data over the course of the experiment. At the beginning of the run, when the bed was still building up, the initial underflow sample had a volume fraction of only 0.17 that increases up to 0.23 when the bed height was increased from ~0.05 to 0.1 m. This indicates an increase in sediment concentration with bed height; an effect that has been widely reported and is due to both the increased residence time within the bed and the larger compressive forces exerted on the bed [6]–[8].

Figure 6 shows a colourmap of solids residence time vs bed height during the experiment calculated using the algorithm described in Equations 1 – 5. The solids residence time of the underflow reaches a maximum at ~9000 s when the bed height is at a maximum as would be expected. To confirm that the residence times estimated were reasonable, using a bed height of 0.175 m and an estimated bed concentration of 508 g l^{-1} from the underflow concentrations, the residence time in the bed from the mass balance was calculated to be 3757 s; in good agreement with the value of ~3250 s at steady state found using the volume-balance model (Equations 1-13). It does, however, indicate the need to carefully select C_Z for this model so that the calculated residence times are realistic.

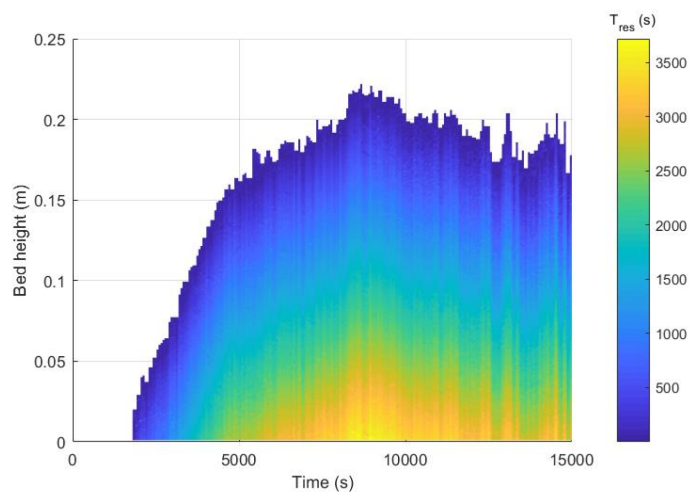

Figure 6) Solids residence time as a function of bed height measured using the ABS for all times where the bed level was above the height of the underflow cone calculated from the volume-balance model (equations 1-13*, for C_z 400 g l^{-1}). The 1 MHz probe was mounted at 0.05 m bed height*

Realistically, the value of C_Z should also be selected as a known initially settled layer concentration, typically assumed by other authors to be the gel point of the suspension [6]. Here the value of C_Z was selected such that the modelled output concentration (shown in Figure Figure *7*) would match the sample concentrations. In order to determine the validity of these results the mass balance at the outlet was performed (equations **12** and **13**) to calculate the predicted outlet concentration at each time step and the results compared to sample data in Figure Figure *7*. The velocity of the particles due to sedimentation and compression ($dh\_compression$) was found to be negative (downward) for nearly all times steps throughout the experiment as would be expected if particles do not move upward in the bed. Some positive values were seen as the bed initially built up likely due to bed slope causing an overestimation of the increase in bed height with time, causing a corresponding overestimation of $dh\_compression$ (equation **6**). This overestimation is then carried through to the model concentration calculation leading to significantly underestimated concentrations at time steps before ~2000 s.

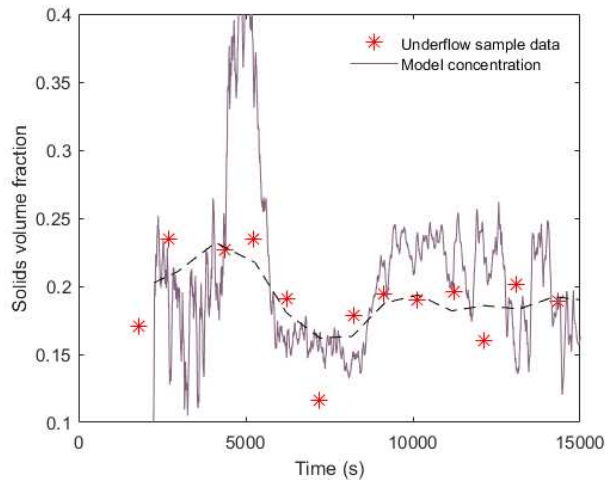

Figure 7 Sample data (3-point moving average) and mass/volume balance model data (10-minute moving average) for laboratory scale thickener outlet concentration vs time

Overall Figure Figure *7* shows fairly good agreement between the mass balance predictions for the outlet concentration and the sample data. Although there is significant variation in the model data due to changes in bed slope and bed disturbances, caused by sudden changes in the underflow rate and sampling, values predicted by the model follow a similar trend to sample data. In particular, a disturbance due to the increased underflow at ~5200 s can be seen as the bed moved down at a higher rate than would be predicted likely due to temporary rheological changes in the bed from the increased flow rate. Despite these disturbances the tracking of the bed height with the ABS is shown here to be able to effectively detect compression and hold-up events in the bed and allow for relatively accurate model estimation of the thickener outlet concentration.

An increase in the value given for C_Z increased the predicted outlet concentration value for the model (equation **13**); an effect that is more significant at early timesteps when the underflow rate was low as the value of $dh_{compression}/Q_u$ was larger and so C_{out} was more sensitive to C_Z (equation **13**). The solids flux through the column during steady-state operation, determined by mass balance based on slurry feed samples, was found to be 0.094 t $hr^{-1}m^{-2}$.

Figure Figure *8*(a) shows attenuation through the settling zone for the vertically facing 2 MHz probe averaged over 4 – 8 cm in front of the probe face with a moving average window of 60 seconds.

Although there are fluctuations seen in the attenuation value, caused by having to move the probe periodically up as the height of the bed increased, it is relatively constant with time for the period of steady state operation (~9000 – 12000 s). Were particle size or concentration to increase there would be an increase in the backscattered signal at short distances and the signal would attenuate more rapidly with increasing distance from the probe [5, 19]. In this way qualitative information about changes to conditions in the feedwell, such as flocculant dosage or particle concentration, could be determined and used to optimise the flocculation process applied to the feed in an industrial application.

Figure 8(b) shows the horizontal attenuation through the settled bed obtained using the 1 MHz probe at a height of 0.05 m above the column base. Attenuation values were determined over a range from 0.03 to 0.06 m (as indicated in Fig. 1) to avoid the noise threshold of the probe at which the backscattered pressure is too low to cause a linear piezoelectric response due to material resistances when converting the acoustic echo to a voltage [19, 34]. Attenuation values seen by the 1 MHz probe in the bed were greater than an order of magnitude larger than those seen with the 2 MHz probe in the settling zone. Given a feedwell diameter of 0.1 m, a feedwell concentration of 60 g l^{-1} and a tank diameter of 0.3 m the concentration in the tank, diluted due to the increase in cross-sectional area, was found to be 6.7 g $l^{`1}$ compared to the ~525 g l^{-1} bed concentration from sampling. Thus, the observed difference in attenuation can be attributed to the much greater sediment concentration within the bed.

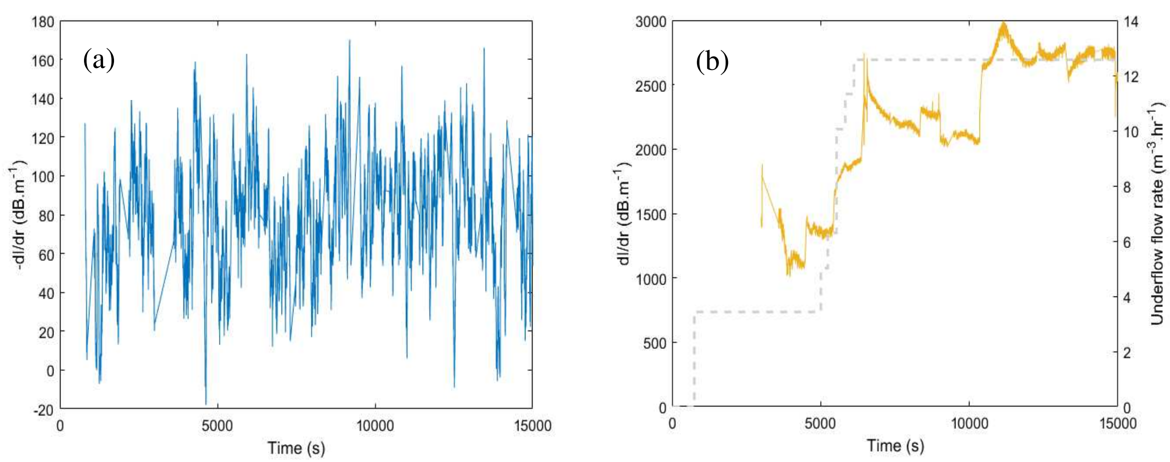

Figure 8 ABS signal attenuation a) through the settling zone for the 2 MHz probe vs time, and b) through the settled bed for the 1 MHz probe with underflow flow rate on the secondary y-axis

The rapid changes in attenuation at 15-minute intervals are due to sample collection at the underflow, causing a sudden disturbance in the bed and the section therefore seen by the probe. Both increases and decreases in attenuation are seen due to this disturbance, however as heterogeneity in the bed structure can cause a bed layer of significantly higher or lower particle concentration to suddenly replace the layer measured by the probe, these rapid changes, while difficult to account for completely, actually highlight the sensitivity of the measurement. It is also noted that, increases in attenuation should translate directly to greater bed density, although while the correlation is linear within a certain region, it is not known whether the high densities of the consolidated bed are outside of this range [19, 20]. Despite these disturbances, there is an apparent clear overall trend observed between the horizontal attenuation and the underflow rate (again shown on the right-hand axis) which is correlated to the overall bed height changes (see Fig. 5). Here, the average attenuation (accounting for sampling disturbances) increases until the bed height is equilibrated, and then remains fairly constant with time.

As the bed height increases, the compressive forces and residence time of the layer measured by the probe increase (see Figure 6 (a) at a height of 0.05 m from the column base). The increased bed volume above the measurement zone increases the dewatering of the suspension and therefore leads to an increase in the acoustic attenuation at that height. This result demonstrates the ability of the ABS to both qualitatively track changes in bed densification through the thickener, while giving insight into the effects of such processes as sampling and raking on sediment bed structure.

Nevertheless, it does also appear, when looking at the underflow sample data, that the attenuation results do not correlate directly. While it is evident that the overall bed concentration decreases after the underflow rate is turned up, this effect is not seen by the ABS attenuation results. This discrepancy is because, although the residence time in the upper section of the bed becomes higher over time, as can be seen in Figure 6, the residence time in the conical section reduces to one third of its original value (~16000 s when the bed depth is equal to the cone height) and so the total residence time within the bed reduces, decreasing the extent of dewatering overall, as measured at the outlet [6].

If multiple probes were placed along the vertical axis facing horizontally into the settled bed, it would be possible to directly infer a density profile through the settled bed, and therefore assess and optimise thickener performance in real-time where sampling would be hazardous, costly or in processes where rapid response times are needed due to unpredictable feed characteristics. For ABS measurements performed by Hunter *et al.* [19] in the same experimental setup, taken vertically through the bed, the signal was only able to penetrate 70 mm into the bed and the attenuation was found to be depth dependent and so attenuation measurements could only be compared for the same bed depth. The influence of bed depth on the acoustic attenuation seen by Hunter *et al.* [19] can be eliminated, however, by taking horizontal measurements through the bed at multiple bed heights and therefore the distance through the bed that the acoustic signal must travel will be the same for each measurement allowing the effect of bed height and depth on acoustic attenuation, and hence sediment concentration, to be isolated.

Conclusions

It has been shown that *in-situ* ABS measurements can be used to track a laboratory thickener bed height, simultaneously to changes in the bed density at a certain level, through measurement of the attenuation of acoustic signal with distance. The residence time in the bed, determined from a transitive volume-balance model to be ~3250 s, was seen to agree well with the value determined from the mass balance (3757 s) for steady state operation, corresponding to a measurement time of ~9000 – 12000 s. Output concentrations using the model were similar to the values determined through sampling and demonstrate the ability to model output thickener concentration using continuous bed height measurements taken using a single vertically facing ABS probe. By using horizontally mounted ABS probes at various heights to measure concentration through the bed, while tracking bed height and signal attenuation in the settling zone and the surface of the bed using a vertically mounted probe, it would be possible to optimise thickening and other dewatering processes in real-time. Such data could be used in acoustic, [5, 16] CFD [11, 26] and settling models [6, 7] to enable comparison of model data to *in-situ* process data and aid in the dewatering and transport of legacy nuclear wastes.

References

[1] D. Carlisle and K. Adamson, "Fuel Pond Sludge –- Lessons Learned from Initial Desludging of Sellafield's Pile Fuel Storage Pond," in *WM2012 Conference*, 2012.

[2] T. Calvin, "Decommissioning Sellafield's First Fuel Storage Pond," *WM2011 Conf.*, 2011.

[3] M. Johnson, J. Peakall, M. Fairweather, S. Biggs, D. Harbottle, and T. N. Hunter, "Characterization of Multiple Hindered Settling Regimes in Aggregated Mineral Suspensions," *Ind. Eng. Chem. Res.*, vol. 55, no. 37, pp. 9983–9993, 2016.

[4] A. Morse, "National Audit Office Report: Managing Risk Reduction at Sellafield," 2012.

[5] P. D. Thorne and D. M. Hanes, "A review of acoustic measurement of small-scale sediment processes," *Cont. Shelf Res.*, vol. 22, no. 4, pp. 603–632, Mar. 2002.

[6] S. P. Usher and P. J. Scales, "Steady state thickener modelling from the compressive yield stress and hindered settling function," *Chem. Eng. J.*, vol. 111, no. 2–3, pp. 253–261, Aug. 2005.

[7] S. P. Usher, R. Spehar, and P. J. Scales, "Theoretical analysis of aggregate densification: Impact on thickener performance," *Chem. Eng. J.*, vol. 151, no. 1–3, pp. 202–208, Aug. 2009.

[8] R. Spehar, A. Kiviti-Manor, P. Fawell, S. P. Usher, M. Rudman, and P. J. Scales, "Aggregate densification in the thickening of flocculated suspensions in an un-networked bed," *Chem. Eng. Sci.*, vol. 122, pp. 585–595, Jan. 2015.

[9] P. Grassia, Y. Zhang, A. D. Martin, S. P. Usher, P. J. Scales, A. H. Crust, and R. Spehar, "Effects of aggregate densification upon thickening of Kynchian suspensions," *Chem. Eng. Sci.*, vol. 111, pp. 56–72, May 2014.

[10] P. J. Scales, A. Kumar, B. B. G. van Deventer, A. D. Stickland, and S. P. Usher, "Compressional dewatering of flocculated mineral suspensions," *Can. J. Chem. Eng.*, vol. 93, no. 3, pp. 549–552, Nov. 2014.

[11] A. R. Heath and P. T. L. Koh, "Combined Population Balance and CFD Modelling of Particle Aggregation by Polymeric Flocculant," in *Third International Conference on CFD in the Minerals and Process Industries*, 2003, pp. 339–344.

[12] P. Garrido, R. Bürger, and F. Concha, "Settling velocities of particulate systems: 11. Comparison of the phenomenological sedimentation–consolidation model with published experimental results," *Int. J. Miner. Process.*, vol. 60, no. 3–4, pp. 213–227, Dec. 2000.

[13] F. A. Benn, P. D. Fawell, J. Halewood, P. J. Austin, A. D. Costine, W. G. Jones, N. S. Francis, D. C. Druett, and D. Lester, "Sedimentation and consolidation of different density aggregates formed by polymer-bridging flocculation," *Chem. Eng. Sci.*, vol. 184, no. 20, pp. 111–125, Jul. 2018.

[14] C. Sahin, R. Verney, A. Sheremet, and G. Voulgaris, "Acoustic backscatter by suspended cohesive sediments: Field observations, Seine Estuary, France," *Cont. Shelf Res.*, vol. 134, pp. 39–51, Feb. 2017.

[15] P. A. Vanrolleghem, B. D. Clercq, J. D. Clercq, M. Devisscher, D. J. Kinnear, and I. Nopens, "New measurement techniques for secondary settlers: A review," *Water Sci. Technol.*, vol. 53, no. 4–5, pp. 419–429, 2006.

[16] H. P. Rice, M. Fairweather, T. N. Hunter, B. Mahmoud, S. Biggs, and J. Peakall, "Measuring particle concentration in multiphase pipe flow using acoustic backscatter: generalization of the dual-frequency inversion method.," *J. Acoust. Soc. Am.*, vol. 136, no. 1, pp. 156–169, 2014.

[17] D. Hurther, P. D. Thorne, M. Bricault, U. Lemmin, and J.-M. Barnoud, "A multi-frequency Acoustic Concentration and Velocity Profiler (ACVP) for boundary layer measurements of fine-scale flow and sediment transport processes," *Coast. Eng.*, vol. 58, no. 7, pp. 594–605, Jul. 2011.

[18] R. Weser, S. Wöckel, B. Wessely, and U. Hempel, "Particle characterisation in highly concentrated dispersions using ultrasonic backscattering method," *Ultrasonics*, vol. 53, no. 3, pp. 706–716, 2013.

[19] T. N. Hunter, S. P. Usher, S. Biggs, P. J. Scales, A. D. Stickland, and G. V. Franks, "Characterization of Bed Densification in a Laboratory Scale Thickener, by Novel Application of an Acoustic Backscatter System," *Procedia Eng.*, vol. 102, pp. 858–866, Jan. 2015.

[20] T. N. Hunter, L. Darlison, J. Peakall, and S. Biggs, "Using a multi-frequency acoustic backscatter system as an in situ high concentration dispersion monitor," *Chem. Eng. Sci.*, vol. 80, no. 1, pp. 409–418, Oct. 2012.

[21] M. Kosonen, S. Kauvosaari, S. Gao, and B. Henriksson, "Performance optimization of paste thickening," in *Proceedings of the 20th International Seminar on Paste and Thickened Tailings*, 2017, pp. 13–22.

[22] A. R. Heath, P. A. Bahri, P. D. Fawell, and J. B. Farrow, "Polymer flocculation of calcite: Relating the aggregate size to the settling rate," *AIChE J.*, vol. 52, no. 6, pp. 1987–1994, 2006.

[23] J. . Swift, K. Simic, R. R. . Johnston, P. . Fawell, and J. . Farrow, "A study of the polymer flocculation reaction in a linear pipe with a focused beam reflectance measurement probe," *Int. J. Miner. Process.*, vol. 73, no. 2–4, pp. 103–118, Feb. 2004.

[24] A. F. Grabsch, P. D. Fawell, S. J. Adkins, and A. Beveridge, "The impact of achieving a higher aggregate density on polymer-bridging flocculation," *Int. J. Miner. Process.*, vol. 124, pp. 83–94, Nov. 2013.

[25] R. Bürger, S. Diehl, and I. Nopens, "A consistent modelling methodology for secondary settling tanks in wastewater treatment," *Water Res.*, vol. 45, no. 6, pp. 2247–2260, Mar. 2011.

[26] T. N. Hunter, D. M. J. Cowell, T. Carpenter, S. Freear, J. Peakall, H. P. Rice, A. Tonge, M. Fairweather, and M. Barnes, "Large-scale trials of a real-time acoustic backscatter system for solids concentration measurement during nuclear waste cleanup," in *IEEE International Ultrasonics Symposium, IUS*, 2016.

[27] R. S. Nyström, J. B. Rosenholm, and K. Nurmi, "Flocculation of Semidilute Calcite Dispersions Induced by Anionic Sodium Polyacrylate-Cationic Starch Complexes," *Langmuir*, vol. 19, no. 9, pp. 3981–3986, 2003.

[28] A. R. Heath, P. A. Bahri, P. D. Fawell, and J. B. Farrow, "Polymer flocculation of calcite: Population balance model," *AIChE J.*, vol. 52, no. 5, pp. 1641–1653, 2006.

[29] A. R. Heath, P. A. Bahri, P. D. Fawell, and J. B. Farrow, "Polymer flocculation of calcite: Experimental results from turbulent pipe flow," *AIChE J.*, vol. 52, no. 4, pp. 1284–1293, 2006.

[30] M. Li, D. Wilkinson, and K. Patchigolla, "Determination of non-spherical particle size distribution from chord length measurements. Part 2: Experimental validation," *Chem. Eng. Sci.*, vol. 60, no. 18, pp. 4992–5003, Sep. 2005.

[31] M. Li and D. Wilkinson, "Determination of non-spherical particle size distribution from chord length measurements. Part 1: Theoretical analysis," *Chem. Eng. Sci.*, vol. 60, no. 12, pp. 3251–3265, Jun. 2005.

[32] A. R. Heath, P. D. Fawell, P. A. Bahri, and J. D. Swift, "Estimating average particle size by focused beam reflectance measurement (FBRM)," *Part. Part. Syst. Charact.*, vol. 19, no. 2, pp. 84–95, 2002.

[33] A. E. Sparr and V. Grippi, "Gravity Thickeners for Activated Sludge," *J. (Water Pollut. Control Fed.*, vol. 41, no. 11, pp. 1886–1904, 1969.

[34] M. Smerdon, A. and M. Simmons, S., "Testing the Limits of a Multi-Frequency Acoustic Sediment Profiling Instrument," in *3rd International Conference & Exhibition on "Underwater Acoustic Measurements: Technologies & Results,"* 2009, pp. 532–538.